

# A Natural Gradient Experiment on Solute Transport in a Sand Aquifer: Spatial Variability of Hydraulic Conductivity and Its Role in the Dispersion Process

E. A. SUDICKY

*Institute for Groundwater Research, Department of Earth Sciences, University of Waterloo, Waterloo, Ontario*

The spatial variability of hydraulic conductivity at the site of a long-term tracer test performed in the Borden aquifer was examined in great detail by conducting permeability measurements on a series of cores taken along two cross sections, one along and the other transverse to the mean flow direction. Along the two cross sections, a regular-spaced grid of hydraulic conductivity data with 0.05 m vertical and 1.0 m horizontal spatial discretization revealed that the aquifer is comprised of numerous thin, discontinuous lenses of contrasting hydraulic conductivity. Estimation of the three-dimensional covariance structure of the aquifer from the log-transformed data indicates that an exponential covariance model with a variance equal to 0.29, an isotropic horizontal correlation length equal to about 2.8 m, and a vertical correlation length equal to 0.12 m is representative. A value for the longitudinal macrodispersivity calculated from these statistical parameters using three-dimensional stochastic transport theory developed by L. W. Gelhar and C. L. Axness (1983) is about 0.6 m. For the vertically averaged case, the two-dimensional theory developed by G. Dagan (1982, 1984) yields a longitudinal dispersivity equal to 0.45 m. Use of the estimated statistical parameters describing the  $\ln(K)$  variability in Dagan's transient equations closely predicted the observed longitudinal and horizontal transverse spread of the tracer with time. Weak vertical and horizontal dispersion that is controlled essentially by local-scale dispersion was obtained from the analysis. Because the dispersion predicted independently from the statistical description of the Borden aquifer is consistent with the spread of the injected tracer, it is felt that the theory holds promise for providing meaningful estimates of effective transport parameters in other complex-structured aquifers.

## INTRODUCTION

Contemporary problems of groundwater pollution can involve the movement of highly hazardous chemical or radioactive wastes over considerable distances in unconsolidated geologic deposits. In many cases, these deposits are comprised of a complex array of lenses or strata of essentially unknown geometry and variable chemical and hydraulic properties.

Long-term predictions of waste migration in these subsurface environments usually involves application of some form of the well-known advection-dispersion equation. Advection refers to the average bulk movement of the solute in the flowing groundwater and dispersion describes solute spreading about the mean displacement position caused by local, irregular advective displacements and molecular diffusion. The conventional development of the advection-dispersion equation considers the mechanical mixing caused by local fluctuations in velocity to be analogous to a large-scale Fickian diffusion process (see, for example, Bear [1972]). The dispersion parameter, dispersivity, is then traditionally assumed to be a unique property of the geologic medium at a particular scale of continuum description [Bear, 1972].

Although the strength of the dispersion process is known to depend upon the degree of heterogeneity and spatial structure of the hydraulic properties of an aquifer, the dispersivity is conventionally obtained by calibration of a solution to the advection-dispersion equation to observed concentration patterns. Because sufficient concentration measurements are sometimes unavailable in practical situations and because source boundary conditions are often unknown, a dispersivity

value obtained by model calibration can become highly uncertain. The dispersivity in these cases can only be regarded as a curve-fitting parameter.

Recent developments in the theory of contaminant transport recognize the complexity of groundwater systems by regarding the fundamental physical and chemical properties of earth materials that affect local solute transport as stochastic processes or as spatial random fields. Then by solving a stochastic form of the governing groundwater flow and mass transport equations in which random hydraulic parameters are represented statistically, average macroscale transport parameters are derived for the purpose of making large-scale transport predictions [Gelhar, 1985]. These macroscale parameters are intrinsically related to the statistical parameters describing complex three-dimensional heterogeneity of a medium's hydraulic properties, with the relationship being determined from the solution of the stochastic equations. Examples of the approach are provided by Gelhar *et al.* [1979], Matheron and de Marsily [1980], Güven *et al.* [1984], and Sudicky [1983] for stratified aquifers and by Dagan [1982, 1984], Gelhar and Axness [1983], and Winter *et al.* [1984] for the more general case of complex-structured, three-dimensional systems. Because a macrodispersivity derived from such theoretical approaches has the dispersive effects caused by small-scale fluctuations in the advective velocity embedded in it, it is then possible to pass to a coarser level of description in order to address the long-term, large-scale mass transport problem.

The theoretical works have also shown that the dispersivity of a heterogeneous aquifer will at first grow with the solute residence time and displacement distance as the dispersion process develops, but will approach a constant asymptotic value. Increasing dispersivity with time and travel distance has been observed in field dispersion tests monitored in exception-

Copyright 1986 by the American Geophysical Union.

Paper number 5W4315.  
0043-1397/86/005W-4315\$05.00

al detail over relatively short travel distances [Dieulin, 1980; Sudicky *et al.*, 1983]. Theory suggests that the approach to an asymptotic dispersivity can be slow and may involve travel distances of many tens, or even hundreds of meters in some cases [Dagan, 1982, 1984, 1986; Sudicky, 1983]. It is therefore unlikely that field dispersion tests could be carried out over such distances on a routine basis to provide estimates of dispersion parameters that are applicable to large-scale transport prediction.

Because the recent advances in dispersion theory provide a framework for dispersivity estimation directly from the variability of the hydraulic properties of an aquifer, thereby avoiding some of the problems associated with the traditional model calibration or tracer-test approach, there is a need to conduct experimental work aimed at verification of the theory. My purpose here is to present the results of extensive measurements of the spatial variability of hydraulic conductivity at the site of an elaborate tracer test performed in the Borden aquifer. Specific details concerning the tracer test can be found in part 1 of the series of papers on the Borden experiment [Mackay *et al.*, this issue]. The rate of spread of the tracer predicted by stochastic dispersion theory using independently estimated geostatistical parameters as input will then be compared to the observed spread of the tracer cloud. Although other studies of the spatial variability of hydraulic parameters have been reported in the literature (see for example, Delhomme [1979], Smith [1980], and Hoeksema and Kitani [1985]), the present study is unique because of the extreme detail of the hydraulic conductivity measurements and because these measurements were made at the site of a long-term tracer test.

#### BORDEN TRACER TEST

In late August, 1982, approximately 12 m<sup>3</sup> of a combined chloride and bromide tracer solution was injected into the shallow water table aquifer at Canadian Forces Base Borden, Ontario and allowed to advect under natural gradient conditions. The tracer site is located in a sand quarry which is about 350 m downgradient from an abandoned landfill (site 1, Figure 1). The site of a natural gradient test performed earlier by Sudicky *et al.* [1983] is located about 200 m west of the present site (site 2, Figure 1). The aquifer is comprised of primarily horizontal, discontinuous lenses of medium-grained, fine-grained, and silty fine-grained sand. There are also infrequent silt, silty-clay, and coarse sand layers. The zone of fluctuations of the water table at the tracer site varies seasonally within about a 1.0 m interval below ground surface.

Following injection of the tracer solution into a zone between 2.0 and 3.6 m below ground surface, three-dimensional tracking of the tracer plume was carried out in exceptional detail using an array of 275 manually installed multilevel sampling devices (Figure 2). Details concerning the construction and installation of the sampling devices are described by Mackay *et al.* [this issue] in part 1 of this series. Each device permits water samples to be extracted from 14–18 discrete points over depth, with the vertical sampling interval varying between 0.2 and 0.3 m.

Hydraulic heads at the tracer site were monitored periodically using an array of piezometers situated at various depths in the aquifer. Contours of the watertable position measured on August 10, 1984, and November 15, 1984, are also shown in Figure 2. The shape of the hydraulic head contours, produced by linear interpolation from about 20 observation

points within the sandpit, indicates that the hydraulic head field at the tracer site is relatively smooth and uniform, although the aquifer is known to be heterogeneous. A horizontal gradient determined from the August 10th measurements is about  $5.6 \times 10^{-3}$  (N54°E orientation), which is 1.6 times greater than the value obtained from the late fall measurements ( $3.6 \times 10^{-3}$ , N40°E orientation). This oscillation in the magnitude and direction of the horizontal hydraulic gradient at the experimental site agrees with that determined from more widely spaced head measurements collected during 11 monitoring episodes in 1979 (MacFarlane *et al.*, [1983]; see also Figure 3, part 1, Mackay *et al.* [this issue]). The annual mean magnitude and orientation of the hydraulic gradient at the injection site is estimated to be about  $4.3 \times 10^{-3}$  and N45°E, respectively, using both the 1979 and 1984 monitoring data. The average vertical gradient appears to be downward on the basis of the vertical movement of the tracer plume, but its value is so small that its detection is difficult using multi-level piezometers.

As of May 31, 1984, over 18,700 individual groundwater samples were collected for chemical analyses and complete three-dimensional spatial coverage of the tracer cloud was obtained for 12 sampling sessions. During the 647-day period of monitoring, the center of mass of the plume had travelled about 58 m, giving a bulk migration rate equal to about 0.09 m/day [Freyberg, this issue]. Isochlors of the vertically averaged chloride concentration after 462 days of movement are shown in Figure 3. It can be seen from Figure 3 that the vertically averaged tracer plume evolved into a relatively smooth, bivariate Gaussian shape with the long, narrow shape of the plume indicating that longitudinal dispersion in the Borden aquifer is substantially stronger than that in the horizontal transverse direction. The vertical spreading of the plume was observed to be very weak and appears to be con-

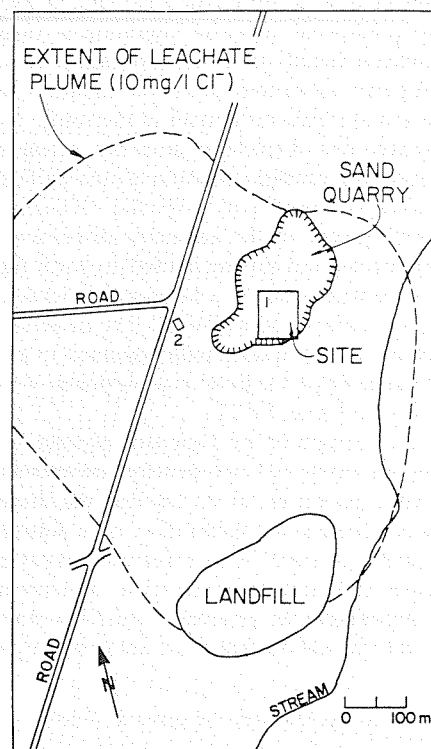


Fig. 1. Location of the Borden tracer site.

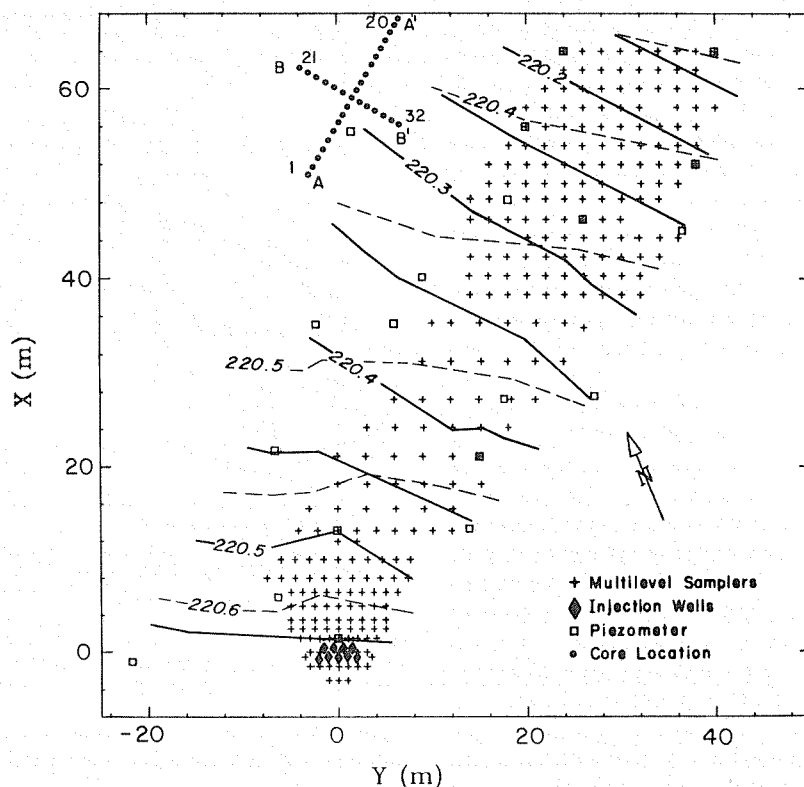


Fig. 2. Instrumentation, location of cores, and hydraulic head distribution on August 10, 1984 (solid curves) and November 15, 1984 (dashed curves), at the tracer test site.

trolled mainly by a local dispersion coefficient on the order of molecular diffusion on the basis of the small overall increase in the vertical extent of the plume [Mackay *et al.*, this issue, Figure 9]. This is consistent with the results of a tracer test performed in 1978 at site 2 located nearby [Sudicky *et al.*, 1983].

#### CHARACTERIZATION OF THE TRACER PLUME

The spatial moments of concentration distributions provide an appropriate means for evaluating the advective and dispersive characteristics of tracer plumes migrating in complex aquifer systems. Estimates of the spatial moments up to second order for the Borden tracer plume have been obtained by Freyberg [this issue] using a quadrature-based numerical integration technique. An overview of his findings are presented below because the plume scale transport parameters arrived at from the moment analysis will be compared later to those deduced from the detailed hydraulic conductivity measurements. The  $ijk$ th moment of a concentration distribution is defined by Freyberg according to

$$M_{ijk} = \iiint_{-\infty}^{\infty} x^i y^j z^k n c \, dx \, dy \, dz \quad (1)$$

where  $c = c(x, y, z, t)$  is the concentration, and  $n$  is the mean porosity. The field coordinate system is that shown in Figure 2, with  $z$  being vertically downward. Using (1), Freyberg further defines, for example,

$$\begin{aligned} M_{000} &= \text{mass of solute in solution;} \\ X_c &= M_{100}/M_{000} \quad \text{x coordinate of center of mass;} \\ Y_c &= M_{010}/M_{000} \quad \text{y coordinate of center of mass;} \end{aligned}$$

$$\begin{aligned} Z_c &= M_{001}/M_{000} \quad \text{z coordinate of center of mass;} \\ \sigma_{xx}^2 &= M_{200}/M_{000} - X_c^2 \quad \text{spatial variance about } X_c; \\ \sigma_{xy}^2 &= M_{110}/M_{000} - X_c Y_c \quad \text{covariance in the x-y plane.} \end{aligned}$$

Additional spatial variance and covariance terms describing the plume can be defined analogously.

It is conventional to define the components of the mean tracer velocity  $v_x$ ,  $v_y$ , and  $v_z$  according to

$$v_x = dX_c/dt \quad v_y = dY_c/dt \quad v_z = dZ_c/dt \quad (2)$$

and the dispersion tensor according to

$$D_{ij} = \frac{1}{2} \frac{d\sigma_{ij}^2}{dt} \quad i, j = x, y, z \quad (3)$$

The above definition for a dispersion coefficient is consistent with recently developed stochastic models of advective-dispersive transport for application to groundwater systems having complex-structured spatial variations in hydraulic conductivity [e.g., Dagan, 1982; Gelhar and Axness, 1983]. Values for the first moments  $X_c$ ,  $Y_c$ , and  $Z_c$  estimated by Freyberg [this issue] are reproduced here in Figure 4 where they are plotted as a function of the plume residence time. It can be seen from Figure 4 that the rate of translation of the center of mass in the horizontal x-y plane is essentially constant, with velocity components  $v_x = 0.082$  m/day and  $v_y = 0.038$  m/day being representative of mean plume scale conditions [Freyberg, this issue]. The resultant horizontal velocity of the center of mass of the plume is thus 0.09 m/day along a N47°E trajectory (25° clockwise with respect to the field x axis).

The rate of change of the vertical coordinate of the center of mass  $Z_c$  is seen to be nonlinear and indicates that the plume moved downward at a decreasing rate during the first 200–300

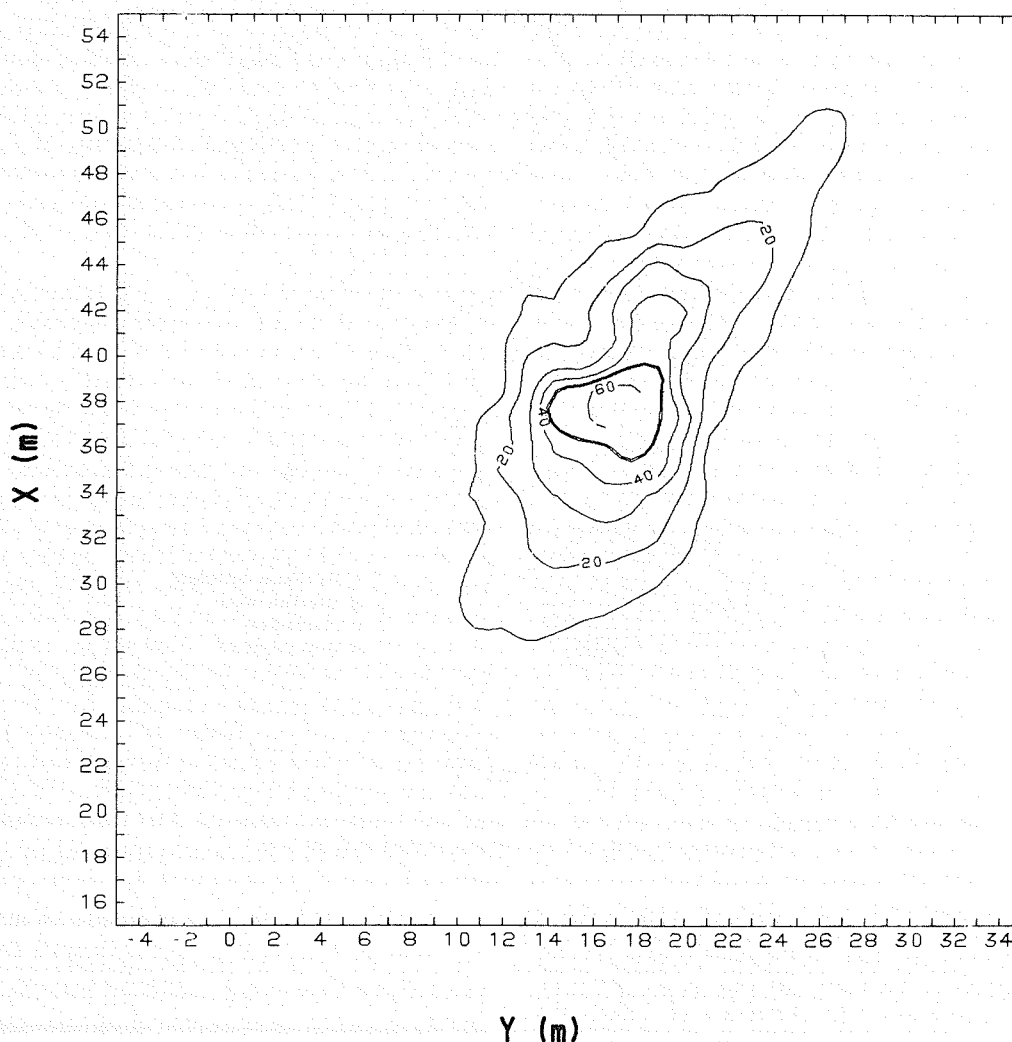


Fig. 3. Vertically averaged chloride concentration (mg/L) after 462 days.

days of transport; however, at larger residence times the downward rate of movement is relatively uniform with constant  $v_z$  equal to about  $10^{-3}$  m/day. The vertical velocity is thus estimated to be nearly 2 orders of magnitude less than the horizontal value. It is believed that the density contrast between the tracer solution and the ambient groundwater caused the more rapid downward movement of the plume during the early stages of transport and then, at the later times when dispersion gradually reduced the tracer concentration, downward movement became primarily hydraulically controlled.

The components of the spatial variance tensor in the horizontal plane were obtained by averaging the concentration vertically across a 6.0-m-depth interval containing the tracer plume [Freyberg, this issue]. Then, as a first approximation, linear regression lines were fitted to the estimates of  $\sigma_{xx}^2$ ,  $\sigma_{yy}^2$ , and  $\sigma_{xy}^2$  after rotation to an  $(x', y')$  coordinate system where the  $x'$  and  $y'$  axes are oriented along and orthogonal, respectively, to the horizontal plume trajectory. In essence, this assumes that the dispersivity is constant and representative of an asymptotic state of dispersive mixing. Finally, using (3) to estimate the directional dispersion coefficients from the fitted lines, the macrodispersivity tensor was obtained by Freyberg

[this issue] from the relationship

$$A_{ij} = D_{ij}/\bar{v} \quad i, j = x, y \quad (4)$$

where  $\bar{v} = 0.091$  m/day is the magnitude of the resultant mean tracer velocity determined from the first-moment results. This simplified analysis yielded the following macrodispersivity values:

$$\begin{bmatrix} A_{11} & A_{12} \\ A_{22} & A_{22} \end{bmatrix} = \begin{bmatrix} 0.36 \text{ m} & 0.023 \text{ m} \\ 0.023 \text{ m} & 0.039 \text{ m} \end{bmatrix} \quad (5)$$

These values for  $A_{11}$  and  $A_{22}$  ( $A_{x'x'}$  and  $A_{y'y'}$ , using Freyberg's notation) represent the traditional longitudinal and horizontal transverse dispersivities, respectively, to describe the spreading along and perpendicular to the mean flow direction.

The magnitude of the longitudinal dispersivity is seen to be at the low end of the range of dispersivities obtained by fitting models to field cases of contamination [Anderson, 1979], but is also much larger than values commonly obtained by passing a tracer through a laboratory column containing homogeneous sand. Because mechanically induced mixing in a homogeneous sand is of the same order as molecular diffusion at low-flow velocities such as those encountered at Borden

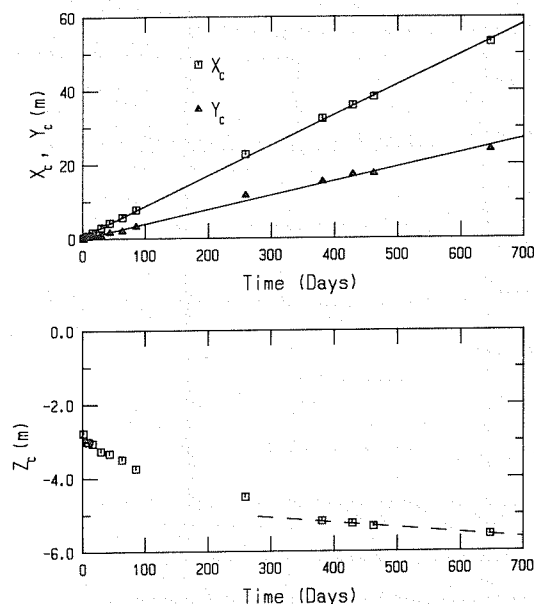


Fig. 4. Center of mass coordinates of the tracer plume versus time [after Freyberg, this issue].

[Bear, 1972], the enhanced dispersion of the tracer slug is believed to be primarily the result of heterogeneity existing in the Borden aquifer.

It should be noted that diagonalization of the dispersivity tensor (5) requires a horizontal rotation equal to about  $30^\circ$  clockwise with respect to the field  $x$  axis giving a principal longitudinal value equal to 0.38 m and a principal transverse value equal to 0.037 m; however, the trajectory of the plume is oriented about  $25^\circ$  clockwise. One reason for this angular offset can be attributed to the configuration of the injection wells. As is described by Freyberg [this issue], the major axis of the plume was oriented along the  $y$  direction following injection which is coincident with the orientation of the two lines of injection wells. With passing time, Freyberg noted that the orientation of the major axis of the plume gradually tended toward the direction of mean flow although it was never completely aligned. Another possible factor contributing to this angular offset between the principal axes of the macrodispersivity tensor and the path followed by the tracer plume is discussed in a later section dealing with estimation of the covariance structure of the hydraulic conductivity field at Borden.

#### SPATIAL VARIABILITY OF HYDRAULIC CONDUCTIVITY

The spatial structure of the hydraulic conductivity field at the tracer test site was investigated by extracting 32 cores of the aquifer material along two core lines, one along the direction of mean groundwater flow ( $A - A'$ ) and one transverse to the mean flow direction ( $B - B'$ ), their locations are shown in Figure 2. A total of 20 cores, each spaced at 1-m horizontal intervals, were obtained along section  $A - A'$ . The transverse core line  $B - B'$  is comprised of 13 cores, again with 1-m horizontal spacings. Core 10 forms the intersection between core lines  $A - A'$  and  $B - B'$ . Each of the cores were approximately 2 m in length and were obtained from depths between about 2.5 and 4.5 m below ground surface. This depth interval is approximately coincident with the vertical extent of the tracer zone.

The field procedure used to obtain the cores first involved percussion-driving a 0.1-m-diameter steel casing to the top of the zone to be cored while wash-boring material from the casing. Once the casing was driven to the desired depth, a thin-walled 0.05-m-diameter aluminum tube serving as the core barrel was inserted into the casing and subsequently percussion driven to the desired depth. Prior to removal of the aluminum core barrel containing the sample, a small suction was applied to the top in order to prevent sample loss from the bottom. Essentially, complete core recovery was obtained in each case. The elevation of the bottom of each core was obtained by careful ground elevation survey and depth measurements.

Each of the cores were carefully opened after cutting the thickness of the aluminum core barrel along the core axis. Visual inspection revealed that the cores were essentially undisturbed and therefore representative of the in situ aquifer material. Examination of the cores further indicated the presence of numerous lenses of coarse to silty fine-grained sand embedded in a fine- to medium-grained sand. The contact between zones having a large textural contrast was usually sharp and near-horizontal across the cores. The thickness of individual beds generally varied from a few centimetres to a few tens of centimetres, with the material within each bed being relatively homogeneous in texture, although fine laminations on the order of a millimetre to a few millimetres thickness were sometimes encountered.

Hydraulic conductivity profiles along each of the 32 cores were obtained as follows. First, each core was subdivided into 0.05 m equal length subsamples and allowed to dry. Because small 0.05 m intervals were chosen, the material within each segment was relatively homogeneous in texture. Each subsample was then placed into a specially designed falling head permeameter that permitted rapid sample emplacement, testing, and removal. Simultaneous use of five permeameters allowed testing of about 75 core subsamples each day. The packing of the material was based on a field estimate for porosity equal to 0.34. This porosity value was obtained from a volumetric analyses of duplicate 0.3 m long cores taken at three locations at the tracer site. Following the passage of  $\text{CO}_2$  through the permeameter, each subsample was saturated with deaired water under upward flow conditions. A hydraulic conductivity value was then determined using the standard falling head procedure. A total of 1279 hydraulic conductivity measurements were made in this manner along the two core lines at the Borden tracer test site.

The permeameter tests were performed at an average room temperature equal to about  $22^\circ\text{C}$  and, except where indicated, all values of hydraulic conductivity reported herein are at this temperature. Because the groundwater temperature at depths corresponding to the cored interval is about  $10^\circ\text{C}$ , a field value for hydraulic conductivity will be about a factor of 1.36 less than a measured value upon viscosity and density corrections.

Although remixing occurs during the emplacement of each 0.05-m subsample into the permeameter device, it is felt that a measured hydraulic conductivity value, after temperature adjustment, is reasonably representative of a local in situ value because each subsample appeared to be relatively homogeneous prior to remixing. The effect on hydraulic conductivity due to repacking to slightly different bulk densities was found to be slight and duplicate tests performed by redrying and



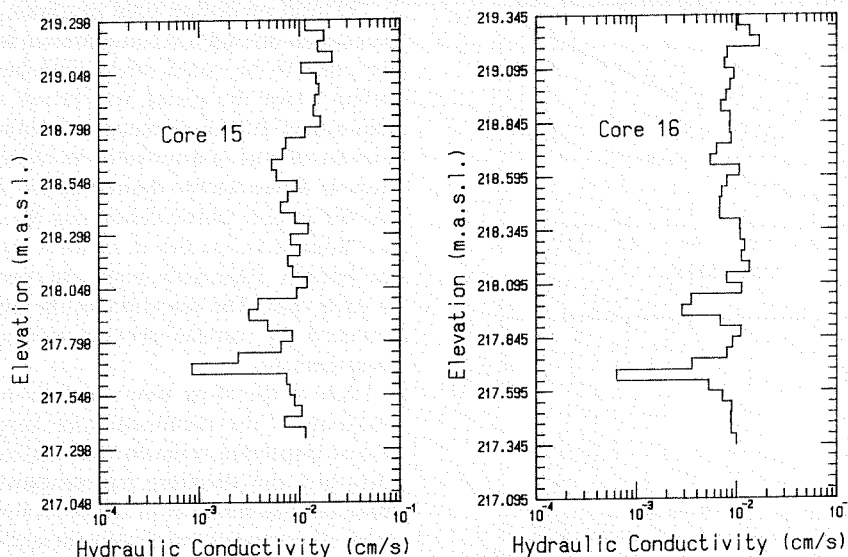


Fig. 5. Comparison of hydraulic conductivity profiles for cores separated by a 1-m horizontal distance.

repacking selected subsamples yielded highly reproducible results.

Figure 5 compares the measured hydraulic conductivity profiles for cores 15 and 16 which are located along core line  $A-A'$  and are separated by a horizontal distance of 1 m. From the results shown in Figure 5, which are typical of the depth variability at the Borden site, it can be seen that the hydraulic conductivity ranges between about  $6 \times 10^{-4}$  and  $2 \times 10^{-2}$  cm/s, which is a contrast in values of slightly more than a factor of 30. The lowest hydraulic conductivity zones for both cores 15 and 16 occur as two individual bands near the bottom of the cores, with the thicknesses of these bands being on the order of 0.1–0.2 m. With the exception of these zones, the hydraulic conductivities range over about a factor of 5. The similarity of the depth profiles for cores 15 and 16 suggest reasonably good horizontal correlation for a 1-m separation distance. There does not appear to be much evidence for a trend in the hydraulic conductivity with depth. This is supported by results from several fully penetrating exploratory cores obtained nearby [Mackay *et al.*, this issue, Figure 4].

Contour plots of the measured hydraulic conductivity field for the two vertical cross sections along  $A-A'$  and  $B-B'$  were produced by linear interpolation and are shown in Figures 6 and 7, respectively. The negative of the natural logarithm of hydraulic conductivity,  $-\ln(K)$ , was contoured because the range of  $-\ln(K)$  is less than that of  $K$ . For contouring purposes, the elevation of each sampling point for hydraulic conductivity shown in Figures 6 and 7 was assigned a value corresponding to the elevation of the midpoint of each 0.05-m core subsample. A total of 720 measurements of hydraulic conductivity with constant vertical (0.05 m) and horizontal (1.0 m) spacing are contained in results for cross-section  $A-A'$ . The total number of data points along  $B-B'$  is 468, with the horizontal and vertical spacing between individual points being the same as that along  $A-A'$ .

Figures 6 and 7 offer a view of the spatial variability of hydraulic conductivity at a scale of unprecedented detail. The results suggest that the Borden aquifer is "homogeneously heterogeneous" over the distal scales that the measurements were performed with the local hydraulic conductivity field having a complex, lenticular structure. Several very distinct but thin

lenses of low hydraulic conductivity are clearly visible along  $A-A'$  (Figure 6) at distances between about 10 and 19 m. The presence of these low hydraulic conductivity zones leads to somewhat greater variability between distances of about 10 and 19 m than over the remainder of the region along  $A-A'$ ; however, on the basis of several exploratory cores taken at various locations throughout the sandpit, it is not felt that this is an indication of the existence of a larger-scale trend in the Borden aquifer.

Given the natural heterogeneity of the Borden aquifer shown in Figure 6 and 7, it can be expected that the local groundwater velocity field will vary irregularly in three-dimensional space over distal scales of a few centimeters to a few tens of centimeters in the vertical direction and over distances on the order of a meter or two in the horizontal plane. It is these scales of velocity fluctuations that are believed to be responsible for the irregularity in the chloride concentration profiles, particularly at early time, that was observed by Mackay *et al.* [this issue] and for the bulk spread of the Borden tracer cloud about its center of mass (dispersion) that was examined by Freyberg [this issue].

A fundamental question that arises is how to deal with this type of material heterogeneity if it is desired to make predictions of solute movement over hundreds of meters as would be the case when modeling the leachate plume emanating from the Borden landfill. Although it is possible to map the structure of dispersion-controlling heterogeneities in some detail over distances of a few metres to a few tens of metres, it would be hopelessly impractical to make detailed measurements of the type performed here over larger distances for the purpose of constructing a detailed deterministic model of the entire aquifer.

Alternatively, the hydraulic conductivity field  $\ln(K)$  can be considered a random field, of which the distribution shown in Figures 6 and 7 is a representative sample with spatial persistence characterized by its covariance function. If this function can be estimated from measurements within the sample domain, then it is possible to estimate the components of the effective hydraulic conductivity and macrodispersivity tensors applicable to the large-scale problem using stochastic theory such as that developed by Gelhar and Axness [1983] and

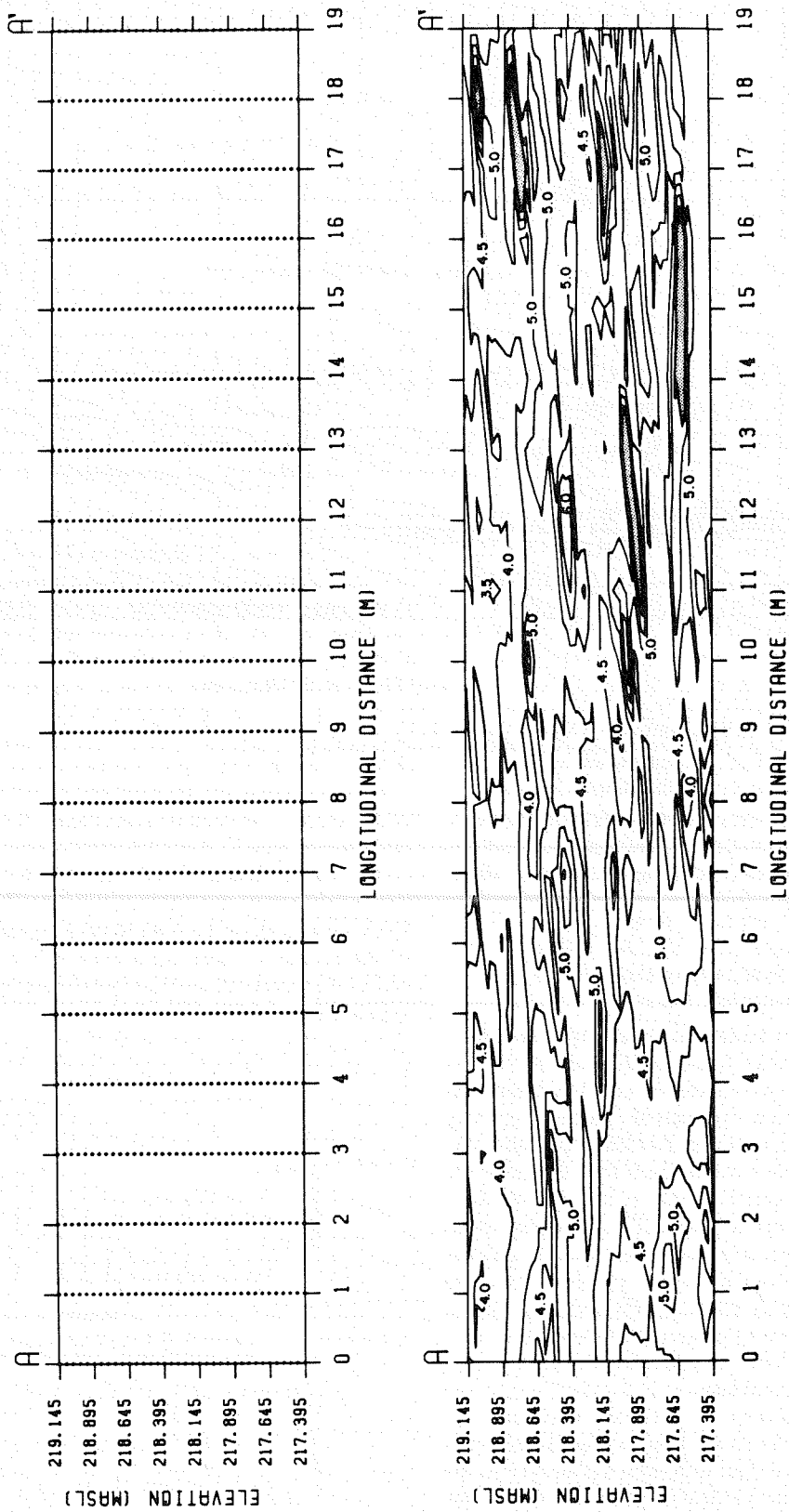


Fig. 6. Location of measurements and distribution of  $-\ln(K)$  along  $A-A'$  (contour interval = 0.5; vertical exaggeration = 2;  $K < 10^{-3}$  cm/s in stippled zones).

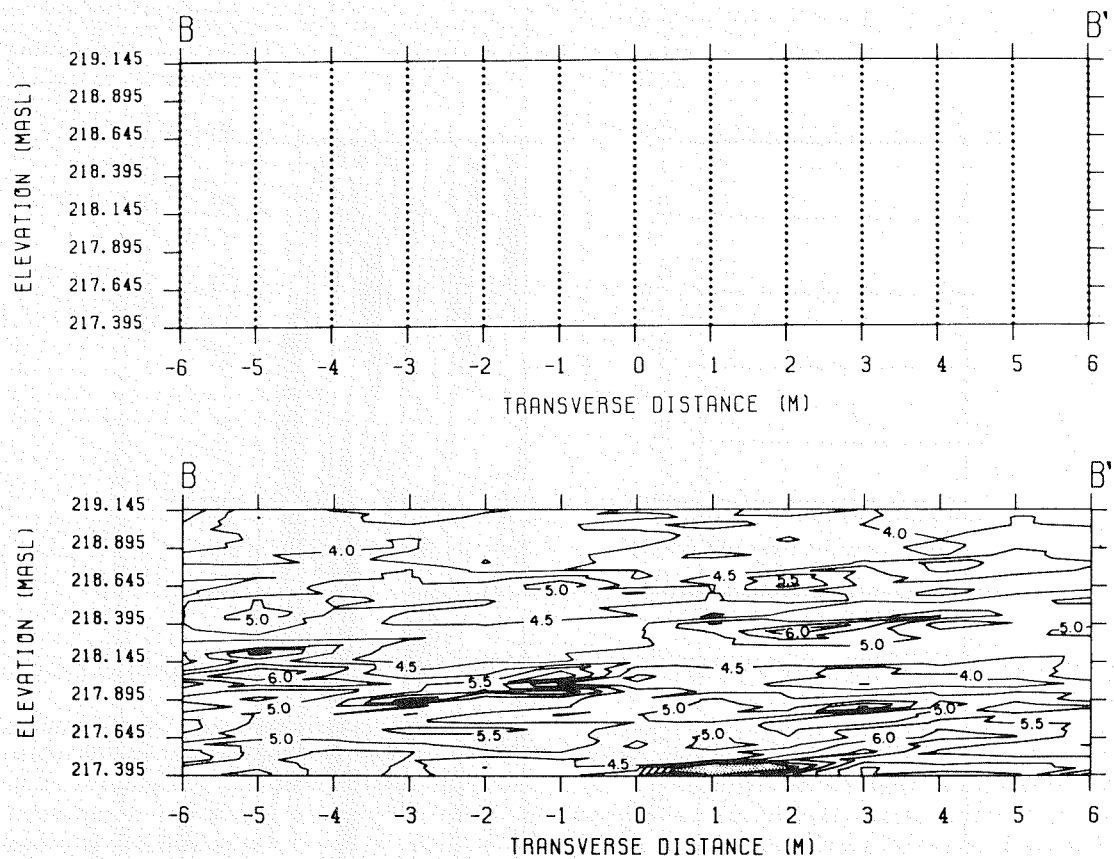


Fig. 7. Location of measurements and distribution of  $-\ln(K)$  along  $B-B'$  (contour interval = 0.5; vertical exaggeration = 2;  $K < 10^{-3}$  cm/s in stippled zone).

Dagan [1982]. In the next section, an estimate of the autocorrelation structure of the Borden aquifer obtained from hydraulic conductivity measurements along the different directions will be presented, and a covariance model for the Borden aquifer will be suggested.

#### CHARACTERIZATION OF THE HYDRAULIC CONDUCTIVITY FIELD

It is normally held that hydraulic conductivity follows a lognormal probability density function [Freeze, 1975]. Frequency histograms of  $Y = \ln(K)$  and  $K$  were constructed by selecting every fifth hydraulic conductivity value from every second core such that the minimum vertical separation distance between adjacent points corresponds to 0.25 m, and the minimum horizontal separation is 2.0 m. Results obtained from one of the many subsets of hydraulic conductivity values separated by these distances are shown in Figure 8. Because hydraulic conductivity values separated by these distances have only weak correlation as will be shown later, the selected values of  $K$  can be considered essentially independent, thus permitting the use of standard statistical tests to either reject or accept the log-normal hypothesis.

Visual inspection of Figure 8 indicates that the log-transformed hydraulic conductivity  $Y$  more closely resembles a Gaussian distribution than that of  $K$  which is skewed to the right. A chi-squared goodness-of-fit test resulted in acceptance of the hypothesis that  $\ln(K)$  comes from a normal distribution, with the probability of mistakenly rejecting the normality hypothesis being less than five percent. Results for a number of other sets of hydraulic conductivity values separat-

ed by a minimum 0.25 m vertical and 2.0 m horizontal spacing were very similar.

The overall mean  $\hat{Y}$  and variance  $\hat{\sigma}_Y^2$  of  $\ln(K)$  at 22°C determined from all 1279 measurements of hydraulic conductivity were found to be  $-4.63$  and  $0.38$ , respectively. The value of the geometric mean  $K_g$  is thus  $9.75 \times 10^{-3}$  cm/s at 22°C. Recall that these values must be reduced by a factor of 1.36 for adjustment to a 10°C field temperature.

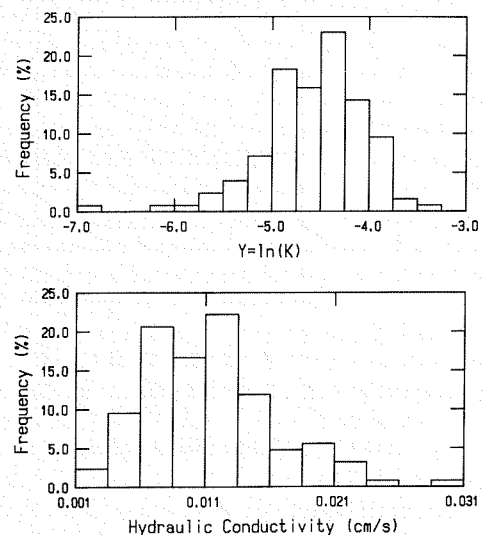


Fig. 8. Frequency histograms for  $\ln(K)$  and  $K$  at the Borden site.



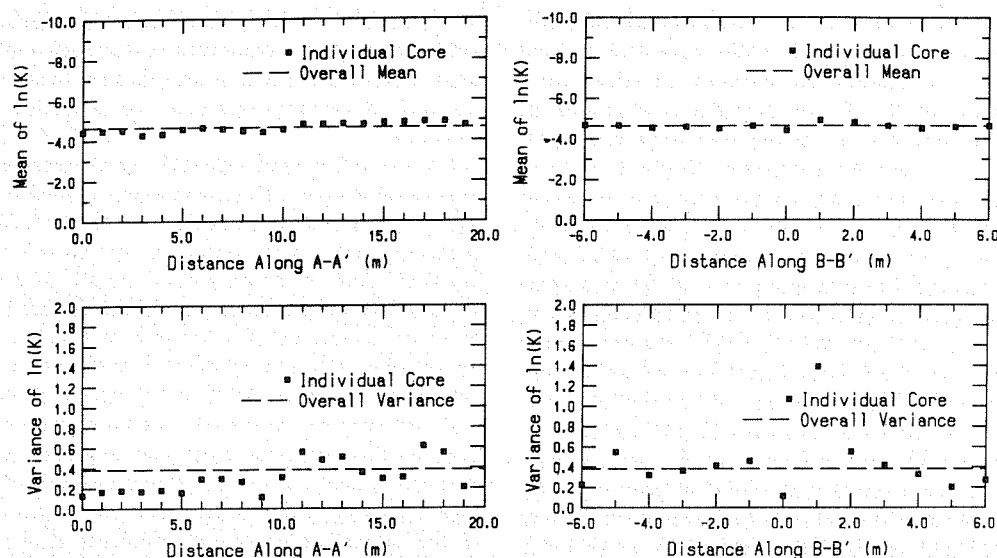


Fig. 9. Mean and variance of  $\ln(K)$  versus distance along  $A - A'$  and  $B - B'$ .

The mean and variance of  $\ln(K)$  determined from each core are plotted with distance along core lines  $A - A'$  and  $B - B'$  in Figure 9 and are compared to the overall mean and variance. Although the mean and variance from each core fluctuate about the overall values, stationarity in the mean and variance of  $\ln(K)$  appears to be a reasonable assumption for the Borden aquifer, at least over the horizontal distances covered by the core lines. The fluctuations in the variance are seen to be larger than that of the mean, with small variance values generally being observed over the first 5 m along  $A - A'$ . These smaller variance values are mainly the result of an absence of thin, low hydraulic conductivity lenses over this distance as can be seen from Figure 6. The largest variance value, equal to about 1.4, occurs at a distance equal to one metre along  $B - B'$  and is the result of measured hydraulic conductivity values in the range of  $5 \times 10^{-5}$  to  $7 \times 10^{-4}$  cm/s over a thin zone near the bottom of core 27.

Horizontal and vertical autocorrelation functions of  $\ln(K)$ ,  $\hat{\rho}_Y$ , were estimated from the equally spaced measurements

along both  $A - A'$  and  $B - B'$  using [Jenkins and Watts, 1968]

$$\hat{\rho}_Y(s_j) = \frac{1}{N} \sum_{i=0}^{N(s_j)} Y'_i Y'_{i+k\Delta s_j} / \frac{1}{N} \sum_{i=0}^N Y_i'^2 \quad k = 0, 1, \dots, m \quad (6)$$

where  $Y' = Y - \hat{Y}$ ,  $N + 1$  is the number of measurements along either  $A - A'$  or  $B - B'$ , and  $k$  is the lag number. The lag-distance increment  $\Delta s_j$  is 0.05 and 1.0 m in the vertical ( $j = 3$ ) and horizontal ( $j = 1, 2$ ), directions, respectively. The results are shown in Figure 10 where they are compared to an exponential model of the form  $\rho_Y(s_j) = \eta \exp(-s_j/\lambda_j)$ .

Because the estimate (6) is normalized with respect to  $\hat{\sigma}_Y^2$ , the parameter  $\eta$  represents the ratio  $\sigma_Y^2/\hat{\sigma}_Y^2$ , where  $\sigma_Y^2 = (\hat{\sigma}_Y^2 - \sigma_0^2)$  is an estimate of the variance of the structured  $\ln(K)$  variability, and  $\sigma_0^2$  is the variance due to essentially uncorrelated variations below the scale of measurement (nugget effect).

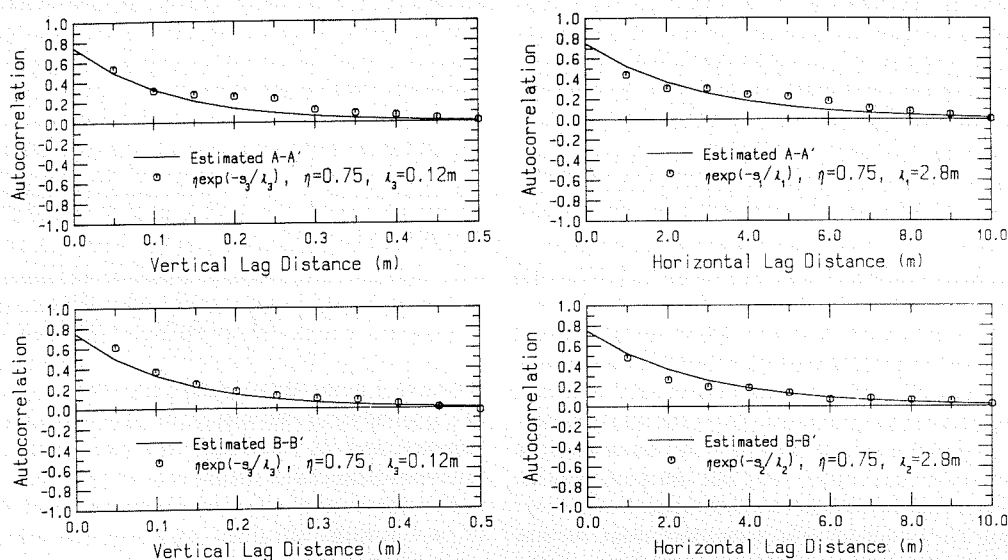


Fig. 10. Vertical and horizontal autocorrelation functions for  $\ln(K)$  along cross-sections  $A - A'$  and  $B - B'$ .

It can be seen from Figure 10 that the exponential model with a vertical correlation length scale  $\lambda_3 = 0.12$  m and  $\eta = 0.75$  closely approximates the estimated vertical autocorrelation function for  $B - B'$  and provides a reasonable fit to that estimated from  $A - A'$ . In the transverse horizontal direction along  $B - B'$ , use of a correlation length  $\lambda_2 = 2.8$  m and  $\eta = 0.75$  provides good agreement with the estimated function, as does use of  $\eta = 0.75$  and  $\lambda_1 = \lambda_2 = 2.8$  m in obtaining the fit with the estimated horizontal correlation function in the longitudinal direction along  $A - A'$ . This suggests isotropy in the correlation structure of the Borden aquifer in the horizontal plane ( $\lambda_1 = \lambda_2$ ). With  $\eta = 0.75$ , the component of the overall variance due to very small-scale variability and any measurement error  $\sigma_0^2$  is estimated to be about 0.09.

The values of the estimated autocorrelation function are believed to be significant over the range of lag distances employed considering, for example, that about 540 pairs of observations are embedded in the value of the estimate for a 4-m lag distance. The fitted values of the parameters  $\eta$  and  $\lambda_j$  fall within the 95% confidence interval of values given by a least square regression performed on the data shown in Figure 10.

The calculation of the autocorrelation function was repeated using the factor  $1/N(s_j)$  instead of  $1/N$  that precedes the first summation in (6) as an alternative estimator [Jenkins and Watts, 1968]. Very similar results were obtained except at large lag distances when  $N(s_j)$  becomes small relative to  $N$ . The calculations were also repeated using  $K$  instead of the log-transformed parameter  $Y$ , again yielding results very similar to those shown in Figure 10.

It has been assumed in the analysis that the horizontal and vertical directions follow the principal correlation axes. Although some of the lenses delineated by the contours shown in Figures 6 and 7 appear to be at a slight angle on the order of  $2^\circ$  or  $3^\circ$  below horizontal, it is felt that little error would be introduced by taking the horizontal and vertical directions as the principal directions of correlation.

Because  $\lambda_1 = \lambda_2 = 2.8$  m was obtained in the horizontal direction along  $A - A'$  and  $B - B'$  and a value for  $\lambda_3 = 0.12$  m is suitable in both cases, and because the mean and variance of  $\ln(K)$  obtained from  $A - A'$  and  $B - B'$  did not differ significantly, the measurements along both core lines can be pooled together to permit estimation of a single horizontal and a single vertical autocorrelation function. When this is done, the resulting directional autocorrelation functions are very close to the average of the individual horizontal and vertical estimates shown in Figure 10 and can be approximated reasonably well by the exponential autocorrelation function with  $\lambda_1 = \lambda_2 = 2.8$  and  $\lambda_3 = 0.12$  m.

The following covariance model  $R(s)$  is therefore suggested to describe the structured  $\ln(K)$  variability in the Borden aquifer

$$R(s) = \sigma_Y^2 \exp \left[ -\left( s_1^2/\lambda_1^2 + s_2^2/\lambda_2^2 + s_3^2/\lambda_3^2 \right)^{1/2} \right] \quad (7)$$

where  $\sigma_Y^2 = 0.75(0.38) = 0.29$ ,  $\lambda_1 = \lambda_2 = 2.8$  m, and  $\lambda_3 = 0.12$  m. It should be recalled that horizontal isotropy in the covariance function is based on the finding that equal horizontal correlation length scales were obtained from the analyses performed along cores lines  $A - A'$  and  $B - B'$ ; however, it is plausible that possible anisotropy was not detected because the two core lines are perpendicular to each other.

Some evidence for statistical anisotropy does exist. As was mentioned previously, the horizontal principal axes of the macrodispersivity tensor (5) are offset by about  $5^\circ$  clockwise

with respect to the plume trajectory. Gelhar and Axness [1983] have shown theoretically that such a displacement will occur in porous media having a statistically anisotropic covariance describing hydraulic conductivity variations (i.e.,  $\lambda_1 = \lambda_2$ ).

On the other hand, there is also evidence in support of horizontal isotropy. First, Nwankwor [1985] performed pumping tests in the Borden aquifer at a nearby location and found radial symmetry of the watertable drawdown about the pumping well. This condition would require isotropy in the bulk average hydraulic conductivity of the aquifer in the horizontal direction which, in turn, implies that  $\lambda_1 = \lambda_2$ . Second, although the hydraulic gradient at the experimental site varies seasonally, its mean direction is nearly coincident with the path followed by the center of mass of the plume. This again suggests that the mean hydraulic conductivity is horizontally isotropic. Finally, Freyberg [this issue] was able to fit the time rate of change of the longitudinal and transverse components of the second-order spatial moments determined from the tracer test using an isotropic covariance for  $\ln(K)$  as input to Dagan's [1982] vertically averaged stochastic transport model. Let us therefore proceed on the basis that the covariance model (7) of the  $\ln(K)$  process is reasonable and try to estimate the principal components of the macrodispersivity tensor from such a description of the aquifer.

#### MACRODISPERSIVITY ESTIMATION USING STOCHASTIC TRANSPORT THEORY

The problem of dispersive mixing caused by a complex flow in three-dimensionally heterogeneous porous media has been addressed in considerable detail by Dagan [1982, 1984], Gelhar and Axness [1983], and Winter et al. [1984] using stochastic continuum theory. Solutions of the perturbed, linearized steady flow and solute transport equations were obtained by Gelhar and Axness using a Fourier-Stieltjes representation of the perturbed quantities and a three-dimensional, anisotropic covariance of  $\ln(K)$  as input. Emphasis was placed on long-term, asymptotic behavior through the use of steady state forms of the governing flow and transport equations. The probabilistic treatment of the dispersion problem by Dagan [1982] is different and is based on the theory of diffusion by continuous movements. Although Dagan's solution is restricted to an isotropic covariance for  $\ln(K)$  and the effect of local dispersion is neglected, he does present expressions relating the time rate of growth of the second moments of the concentration distribution (i.e., spatial spread) to the statistical properties of the hydraulic conductivity field.

A general integral expression of the following form was obtained by Gelhar and Axness [1983] for the asymptotic macrodispersivity tensor:

$$A_{ij} = \iiint_{-\infty}^{\infty} \frac{S_{v_{ij}} d\mathbf{k}}{[i\bar{v}k_1 + D_L^* k_1^2 + D_T^*(k_2^2 + k_3^2)]\bar{v}} \quad (8)$$

where  $S_{v_{ij}}$  is the cross spectrum of the  $i$  and  $j$  components of the groundwater velocity,  $\bar{v}$  is the magnitude of the mean velocity, and  $D_L^*$  and  $D_T^*$  are local-scale longitudinal and transverse dispersion coefficients, respectively.

For the case of isotropy in the plane of the stratification ( $\lambda_1 = \lambda_2$ ), with coordinate axes oriented along ( $x_1$  direction) and orthogonal ( $x_3$  direction) to the direction of  $\bar{v}$ , the following nonzero components of  $A_{ij}$  were obtained from (8) by

Gelhar and Axness [1983]:

$$A_{11} = \sigma_Y^2 \lambda_1 \mu / (\gamma^2 \zeta) \quad (9a)$$

$$A_{22} = \sigma_Y^2 \lambda_1 \mu J_3^2 / [2(1 + \zeta) \gamma^2 J_1^2] \quad (9b)$$

$$A_{33} = \sigma_Y^2 \lambda_1 J_3^2 (1 + 2\zeta) / [2(1 + \zeta) \gamma^2 J_1^2] \quad (9c)$$

$$A_{13} = A_{31} = \sigma_Y^2 \lambda_1 \mu J_3 / [(1 + \zeta) \gamma^2 J_1] \quad (9d)$$

where  $\mu = \lambda_3 / \lambda_1$ ;  $J_1$  and  $J_3$  are the components of the mean hydraulic gradient in the  $x_1$  and  $x_3$  directions, respectively;  $\zeta = (\sin^2 \theta + \mu^2 \cos^2 \theta)^{1/2}$ ; and  $\theta$  is the angle that the mean flow forms with the bedding planes. The flow factor  $\gamma = q / (K_g J_1)$ , with  $q$  being the mean specific discharge, has the form

$$\gamma = \exp [\sigma_Y^2 (\frac{1}{2} - g_{33})] / (\sin^2 \theta + \beta \cos^2 \theta) \quad (10)$$

where  $\beta = \exp [\sigma_Y^2 (g_{11} - g_{33})]$ , and  $g_{ii}$  depends on the correlation scales as defined by Gelhar and Axness. It should be noted that local dispersion (i.e.,  $D_L^*$ ,  $D_T^*$ ) was neglected by Gelhar and Axness in the asymptotic analysis leading to (9).

Before evaluating the components of  $A_{ij}$  from (9), the components of the effective hydraulic conductivity tensor will be determined. These are given by Gelhar and Axness [1983] as

$$\bar{K}_{ii} = K_g \exp [\sigma_Y^2 (\frac{1}{2} - g_{ii})] \quad (11)$$

Using a temperature-adjusted value for the geometric mean hydraulic conductivity  $K_g = 7.17 \times 10^{-3}$  cm/s,  $\sigma_Y^2 = 0.29$ , and appropriate values of  $g_{ii}$  with  $\lambda_1 = \lambda_2$  and  $\lambda_1 / \lambda_3 = 23$ , the following is obtained for a 10°C field temperature:

$$\begin{bmatrix} \bar{K}_{11} & & \\ & \bar{K}_{22} & \\ & & \bar{K}_{33} \end{bmatrix} = \begin{bmatrix} 8.20 \times 10^{-3} \text{ cm/s} \\ 8.20 \times 10^{-3} \text{ cm/s} \\ 6.33 \times 10^{-3} \text{ cm/s} \end{bmatrix} \quad (12)$$

Because the vertical component of the tracer velocity was observed to be almost 2 orders of magnitude smaller than the horizontal component such that flow is predominately along the bedding ( $\lambda_1$ —direction), it is assumed that the components (12) are the principal values of the effective hydraulic conductivity tensor. The anisotropy ratio  $\bar{K}_{11} / \bar{K}_{33}$  is about 1.3. These values for  $\bar{K}_{ii}$  and the anisotropy ratio are reasonably consistent with values obtained by Nwankwor [1985], who performed a series of pump tests in the Borden aquifer at a location near the tracer-test site.

A value for the horizontal component of the groundwater velocity calculated using  $\bar{K}_{11} = 8.20 \times 10^{-3}$  cm/s, a hydraulic gradient  $J_1 = 4.3 \times 10^{-3}$ , and a porosity equal to 0.34 is about 9.0 cm/day. This value is very close to the tracer velocity determined from the moment analysis (9.1 cm/day). The difference is very small considering that observed temporal variations in the hydraulic gradient at the test site are ignored in the above calculation.

In order to compute the macrodispersivity tensor from (9), an estimate of  $J_3$  is required. This was obtained using  $J_3 = nv_z / \bar{K}_{33}$ , where  $n = 0.34$  is the porosity,  $v_z = 0.1$  cm/day, is the vertical component of the tracer velocity estimated from the moment analysis (see Figure 4), and  $\bar{K}_{33} = 6.33 \times 10^{-3}$  cm/s from (12). Thus the estimated value for  $J_3$  is about  $6 \times 10^{-5}$ . Using this value for  $J_3$  and recognizing that the angle  $\theta$  is very small for the system at hand such that  $\sin \theta \simeq 0$  and  $\cos \theta \simeq 1$ ,

the following values for  $A_{ij}$  were estimated from (9):

$$\begin{bmatrix} A_{11} & & A_{13} \\ & A_{22} & \\ A_{31} & & A_{33} \end{bmatrix} = \begin{bmatrix} 0.61 \text{ m} & & \sim 0 \\ & \sim 0 & \\ \sim 0 & & \sim 0 \end{bmatrix} \quad (13)$$

Because both the angle  $\theta$  and  $J_3$  are small, extremely small values for  $A_{22}$ ,  $A_{33}$ , and  $A_{13}$  were obtained. Thus the macrodispersivities  $A_{ij}$  in (13) are considered to be principal values. To account for pore scale dispersion, the predicted  $A_{ij}$  values should be augmented by appropriate values of the local longitudinal and transverse dispersivity. The weak vertical dispersion that is predicted is consistent with the observations made by Mackay *et al.* [this issue] on the vertical extent of the tracer plume and the conclusion made by Sudicky [1983] on the basis of the 1978 tracer test that vertical dispersion in the Borden aquifer is essentially diffusion-controlled.

Because closed-form expressions describing the development of the dispersion process were not presented by Gelhar and Axness [1983], the theory developed by Dagan [1982, 1984] and later extended by G. Dagan (unpublished manuscript, 1986) for the situation at hand will be used to predict the time rate of change of the second moments of the vertically averaged concentration distribution. The principal components of the spatial variance tensor of a tracer cloud,  $\sigma_{11}^2$  in the longitudinal direction and  $\sigma_{22}^2$  in the transverse direction, were found by Dagan to vary with residence time  $t$  according to

$$\sigma_{11}^2 = 0.74(2\sigma_Y^2 \lambda^2) \left\{ \frac{3}{4} - \frac{3}{2} E + \frac{L}{\lambda} + \frac{3}{2} \left[ Ei(-L/\lambda) - \ln(L/\lambda) + \frac{\lambda}{L} \exp(-L/\lambda) \left( 1 + \frac{\lambda}{L} \right) - \frac{\lambda^2}{L^2} \right] \right\} \quad (14a)$$

$$\sigma_{22}^2 = 0.74(2\sigma_Y^2 \lambda^2) \left\{ \frac{3}{2} \left[ \frac{\lambda^2}{L^2} - \frac{\lambda}{L} \left( 1 + \frac{\lambda}{L} \right) \exp(-L/\lambda) \right] - \frac{1}{2} [Ei(-L/\lambda) - \ln(L/\lambda)] - \frac{3}{4} + \frac{1}{2} E \right\} \quad (14b)$$

where  $E = 0.577 \dots$  is the Euler constant;  $\lambda = \lambda_1 = \lambda_2$  is the correlation length of  $\ln(K)$ ;  $L = \bar{v}t$ ; and  $Ei(-x)$  is the exponential integral. The above result is based on a two-dimensional flow representing vertically averaged conditions. Equation (14) differs from Dagan's [1982, 1984] original solution by the addition of the leading constant 0.74 which expresses the approximate relationship between the three-dimensional covariance of  $\ln(K)$  estimated here and that of the vertically averaged  $\ln(K)$  field (G. Dagan, unpublished manuscript, 1986).

Equation (14) was evaluated using the statistical parameters given in the previous section as input and with the calculated  $\bar{v} = 9.0$  cm/day. The results are compared with actual values determined from the field test in Figure 11. Also shown is the best fit prediction obtained independently by Freyberg [this issue] by calibrating (14) to the field data. Standard Cartesian-tensor transformation laws were used to determine the components  $\sigma_{11}^2$  and  $\sigma_{22}^2$  from  $\sigma_{xx}^2$ ,  $\sigma_{yy}^2$ , and  $\sigma_{xy}^2$ , as calculated by Freyberg on the basis of the field  $x$ - $y$  coordinate system shown in Figure 2. It should be noted that field estimates of  $\sigma_{11}^2 = 1.8 \text{ m}^2$  and  $\sigma_{22}^2 = 2.6 \text{ m}^2$  at  $t = 0$  day were added to (14a) and (14b), respectively, to account for the substantial dimensions of the tracer slug following injection. It can be

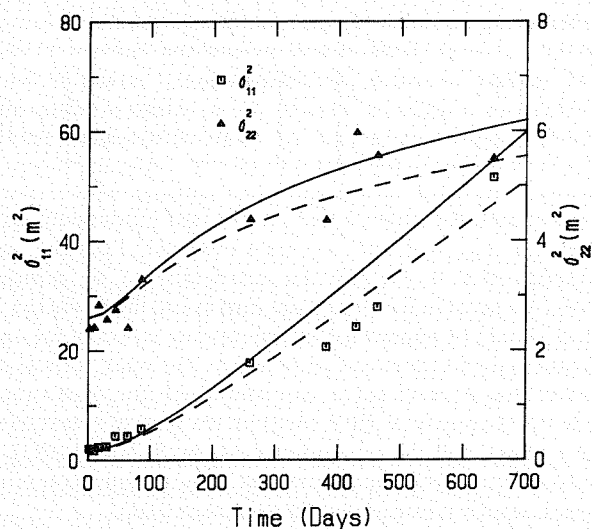


Fig. 11. Comparison of values of the spatial variance tensor in the horizontal plane  $\sigma_{ij}^2$  from field test with those computed from Dagan's [1982, 1984] theory (solid curves). The dashed curves are calibration fits by Freyberg [this issue].

seen from Figure 11 that the theory provides good agreement with the actual spread of the tracer in the longitudinal direction throughout most of the duration of the experiment. The main differences between the theoretical and experimental values of  $\sigma_{11}^2$  occur at 381, 429, and 462 days with the field values of  $\sigma_{11}^2$  at these times being less than those predicted by (14a). Although there is considerable scatter in the field estimates of  $\sigma_{22}^2$ , much of the scatter appears to be centered about the prediction based on (14b). At any rate, the generally favorable comparison was obtained without curve fitting by adjustment of the input parameters.

The calibrated results obtained by Freyberg [this issue] using  $v = 0.091$  m/day,  $\sigma_Y^2 = 0.24$ , and  $\lambda = 2.7$  m as input to (14) are shown as the dashed curves in Figure 11. These values for  $\sigma_Y^2$  and  $\lambda$ , obtained by a trial-and-error procedure until a visual fit with the field data was obtained, are quite close to the values estimated independently here from the observed  $\ln(K)$  variability. Considering the scatter associated with the moment data and the uncertainty associated with estimation of the statistical parameters describing the  $\ln(K)$  variability, each of the predictions shown in Figure 11 are equally acceptable. Because the calibrated  $\sigma_Y^2$  and  $\lambda$  values compare well with the values obtained from the observed  $\ln(K)$  variability and because the early time moment estimates (say,  $t < 300$  days for the Borden test) are sufficient for calibration, it therefore seems that relatively short duration tracer tests can be utilized as a means for inferring these geostatistical parameters. This approach was suggested by Matheron and de Marsily [1980].

Because our main aim is to predict the magnitude of the components of the macrodispersivity tensor from the statistical parameters describing heterogeneity, it is instructive to examine whether or not asymptotic mixing conditions were arrived at in the field test. It can be seen from Figure 11 that values of  $\sigma_{11}^2$  predicted by (14a) increase more slowly at first compared to the rate of increase at later times, thus pointing to an increase of the longitudinal dispersivity with time and travel distance as the solute body first invades the aquifer. After about 500 days of residence time, the relationship (14a)

becomes nearly linear and the longitudinal dispersivity would appear to approach a constant value from a practical standpoint. The distance travelled by the plume after this amount of time is equivalent to about 18 horizontal correlation lengths. The mixing in the horizontal transverse direction, however, appears to be far from asymptotic, since  $\sigma_{22}^2$  values predicted by (14b) grow only logarithmically with time.

The asymptotic form of (14a) when  $t \rightarrow \infty$  leads to a longitudinal macrodispersivity for vertically averaged conditions that are identical to the Gelhar and Axness [1983] three-dimensional result (9a) except for the factor  $0.74/\gamma$ . For the vertically averaged situation, the relationships (3) and (14a) provide a longitudinal macrodispersivity equal to about 0.45 m. There is little difference between this value and the value obtained by Freyberg [this issue] using the calibration approach (0.47 m). Although the values of  $\sigma_{22}^2$  given by (14b) eventually grow logarithmically with time, the derivative of (14b) with respect to time leads to  $A_{22} = 0$  in the long-time limit.

The predicted values of  $A_{ij}$  derived from (14) should also be compared to those estimated by Freyberg [this issue] under the assumption that observed field values  $\sigma_{ij}^2$  are always a linear function of time. The longitudinal macrodispersivity  $A_{11} = 0.45$  m calculated from the two-dimensional Dagan [1986] model (14) is somewhat larger than the value  $A_{11} = 0.36$  m determined from the linear fit to the observed  $\sigma_{11}^2$  data and, in the horizontal transverse direction, a linear fit to the  $\sigma_{22}^2$  data leads to a much larger value for  $A_{22}$  than that predicted by the Dagan model. The fitting of a classic linear model fails to distinguish between early time and large time behavior. Because of this, the early time data would tend to enhance the slope of the fitted  $\sigma_{22}^2$  line and underestimate the slope of the  $\sigma_{11}^2$  line.

There are several factors unaccounted for in either the two-dimensional Dagan [1986] or three-dimensional Gelhar and Axness [1983] theories which could have influenced the observed rate of spread in the horizontal transverse direction. First, as can be seen from Figure 4, a significant downward flow across the strata occurred during the first 200–300 days following injection ( $v_z \approx 10^{-2}$  m/day). If the enhanced downward flow, thought to be the result of density contrasts, is expressed in the form of an effective hydraulic gradient  $J_3$  and the angle of flow  $\theta$  is modified accordingly, then it can be seen from (9) that larger values for  $A_{22}$  and  $A_{13} = A_{31}$  would be obtained. Second, the direction of the hydraulic gradient at the test site was noted to fluctuate seasonally about the direction of the plume trajectory. Ackerer and Kinzelbach [1985] have shown by means of numerical model studies that the resultant temporal variations in the flow field will enhance horizontal transverse dispersion while not significantly increasing the longitudinal mixing process. Because the theories used here rely on the assumption of steady flow conditions, then it would be expected that a theoretical value for  $A_{22}$  which is based only on velocity fluctuations due to material heterogeneity would be less than that determined from a field dispersion test affected by this type of dispersion mechanism. The main features of the enhanced dispersion caused by seasonal flow variations might, however, be handled in a practical yet realistic way by incorporating the flow transients in a transport model, with macrodispersivities of the type estimated here used as input to account for the material heterogeneity.

Although some uncertainty exists concerning the actual



strength of the dispersion process in the horizontal transverse direction for reasons outlined above, the dispersion in this direction is nevertheless relatively weak compared to the longitudinal mixing process in the Borden aquifer. Because the rate of longitudinal dispersion predicted from stochastic theory using input statistical parameters arrived at from an analysis of the measured  $\ln(K)$  variability agrees with the observed rate and because the calculated vertical transverse dispersion is controlled mainly by local-scale dispersion, which is also consistent with experimental observations, it is felt that there is mounting evidence in support of the theory. Further encouragement is provided by the agreement between the mean advection rate computed using the effective macroscale hydraulic conductivity tensor and the value obtained independently from the tracer test.

What remains to be determined is the robustness of such theory when applied to a wide range of geologic media, particularly those having a large variance in  $\ln(K)$ . This points to the need for further elaborate tracer tests performed in various subsurface environments together with extensive measurements of the spatial variability of hydraulic conductivity in each of the geologic settings. Carefully designed detailed numerical simulations of flow and solute transport in media with prescribed statistical properties are also much needed. Work of this nature is currently in progress.

#### CONCLUSIONS

The numerous detailed hydraulic conductivity measurements performed at the site of the Borden tracer test lend support to the contention that the hydraulic properties of an aquifer vary irregularly in three-dimensional space as a general rule. The structure was observed to consist of a complex array of near-horizontal beds of contrasting hydraulic conductivity that vary in thickness from a few centimetres to a few tens of centimeters. Moreover, the layering is clearly discontinuous in the horizontal direction with typical bed lengths being on the order of one to a few meters. These horizontal and vertical hydraulic conductivity variations are most likely responsible for the irregularity in concentration profiles that appeared during the early stages of the field tracer test and for the significant enhancement of the longitudinal dispersion process.

The scale of the dispersion-controlling heterogeneity in the Borden aquifer is small compared to the scale of travel distances that are relevant to the long-term migration of the tracer cloud. It would therefore be unrealistic to perform measurements at every point throughout the entire migration path of the plume in order to capture the subtle, yet important, features of the hydraulic conductivity field. Because of this, variations in the hydraulic properties of earth materials such as those at Borden will be essentially unknown and unpredictable as long as a disparity exists between the scale of the heterogeneity and the scale of the contamination problem in the field.

This difficulty in precisely characterizing the structure of an aquifer should be recognized in the design of field studies of aquifer contamination. I have attempted to illustrate that if statistical parameters coherent with modern stochastic theories of dispersion can be ascertained to describe variability, it is then possible to obtain meaningful estimates of effective large-scale transport parameters. The generally good agreement between the rates of macrodispersion observed during the long-term tracer test and those rates computed

independently from theory using the statistical description of the Borden aquifer as input has demonstrated that workable results are presently at hand.

Further field studies leading to the development of routine and efficient procedures for the estimation of the required statistical parameters, such as geophysical techniques, short-term tracer tests or the combination of pumping test data with results from several vertical cores, are much needed. Ideally, this type of work should be performed in conjunction with long-term tracer tests in a variety of aquifer types. Input from the geologist concerning the depositional history of sediments at each site will be valuable to establish possible generic classification of aquifers with common statistical characteristics according to their geologic origin. Based on the Borden results, there is reason to believe that dispersivity is a measurable quantity that can be obtained by procedures other than arbitrary curve fitting.

*Acknowledgments.* Funding for the acquisition of the spatial variability data and the interpretation of these data was provided to the University of Waterloo through a research contract with Atomic Energy of Canada Limited (AECL), Chalk River Nuclear Research Laboratories, Chalk River, Ontario. The injection part of the tracer experiment and the subsequent sampling and analyses conducted by Waterloo and Stanford personnel were supported by the R. S. Kerr Environmental Research Laboratory of the U.S. Environmental Protection Agency through assistance agreement CR-808851 to Stanford University. The many helpful discussions with D. L. Freyberg of Stanford University, who performed the spatial moment analysis on the tracer plume, J. A. Cherry of the University of Waterloo, and G. L. Moltyaner of AECL are gratefully acknowledged. Correspondence with G. Dagan during the later stages of this work was invaluable. I am indebted to R. Ingleton, hydrogeology technician, and W. Blackport, graduate student, of the University of Waterloo, who together shared the burden of core acquisition and subsequent permeameter testing.

#### REFERENCES

- Ackerer, P., and W. Kinzelbach, Modélisation du transport de contaminant par la méthode de marche au hasard: influence des variations du champ d'écoulement au cours du temps sur la dispersion, paper presented at Proceedings, International Association of Hydraulic Research Symposium on the Stochastic Approach to Subsurface Flow, Int. Assoc. of Hydraul. Res., Montvillargenne, France, June 1985.
- Anderson, M. P., Using models to simulate the movement of contaminants through groundwater flow systems, *CRC Crit. Rev. Environ. Control*, 9(2), 97-156, 1979.
- Bear, J., *Dynamics of Fluids in Porous Media*, Elsevier Science, New York, 1972.
- Dagan, G., Stochastic modeling of groundwater flow by unconditional and conditional probabilities, 2, The solute transport, *Water Resour. Res.*, 18(4), 835-848, 1982.
- Dagan, G., Solute transport in heterogeneous porous formations, *J. Fluid Mech.*, 145, 151-177, 1984.
- Dagan, G., Statistical theory of groundwater flow and transport: Pore to laboratory, laboratory to formation, and formation to regional scale, *Water Resour. Res.*, 22(9), 120S-134S, 1986.
- Delhomme, J. P., Spatial variability and uncertainty in groundwater flow parameters: A geostatistical approach, *Water Resour. Res.*, 15(2), 269-280, 1979.
- Dieulin, A., Propagation de pollution dans un aquifère alluvial, l'effet de parcsours, Thèse de Docteur-Ingénieur, l'Université Pierre et Marie Curie-Paris VI, 1980.
- Freeze, R. A., A stochastic-conceptual analysis of one-dimensional groundwater flow in nonuniform homogeneous media, *Water Resour. Res.*, 11(5), 725-741, 1975.
- Freyberg, D. L., A natural gradient experiment on solute transport in a sand aquifer, 2, Spatial moments and the advection and dispersion of nonreactive tracers, *Water Resour. Res.*, this issue.
- Gelhar, L. W., Stochastic subsurface hydrology from theory to applications, *Water Resour. Res.*, 22(9), 135S-145S, 1986.



- Gelhar, L. W., and C. L. Axness, Three-dimensional stochastic analysis of macrodispersion in aquifers, *Water Resour. Res.*, 19(1), 161-170, 1983.
- Gelhar, L. W., A. L. Gutjahr, and R. L. Naff, Stochastic analysis of macrodispersion in a stratified aquifer, *Water Resour. Res.*, 15(6), 1387-1396, 1979.
- Güven, O., F. J. Molz, and J. G. Melville, An analysis of dispersion in a stratified aquifer, *Water Resour. Res.*, 20(10), 1337-1354, 1984.
- Hoeksema, R. J., and P. K. Kitanidis, Analysis of the spatial structure of properties of selected aquifers, *Water Resour. Res.*, 21(4), 563-572, 1985.
- Jenkins, G. M., and D. G. Watts, *Spectral Analysis and its Applications*, Holden-Day, San Francisco, Calif., 1968.
- MacFarlane, D. S., J. A. Cherry, R. W. Gilham, and E. A. Sudicky, Migration of contaminants at a landfill: A case study, 1, Groundwater flow and plume delineation, *J. Hydrol.*, 63, 1-29, 1983.
- Mackay, D. M., D. L. Freyberg, P. L. McCarty, P. V. Roberts, and J. A. Cherry, A natural gradient experiment on solute transport in a sand aquifer, 1, Approach and overview of plume movement, *Water Resour. Res.*, this issue.
- Matheron, G., and G. de Marsily, Is transport in porous media always diffusive? A counter-example, *Water Resour. Res.*, 16(5), 901-917, 1980.
- Nwankwor, G., Delayed yield processes and specific yield in a shallow sand aquifer, Ph.D. thesis, Univ. of Waterloo, Waterloo, Ont., 1985.
- Smith, L., Spatial variability of flow parameters in stratified sand, *Int. J. Math. Geol.*, 13(1), 1-21, 1980.
- Sudicky, E. A., An advection-diffusion theory of contaminant transport for stratified porous media, Ph.D. thesis, Univ. of Waterloo, Waterloo, Ont., 1983.
- Sudicky, E. A., J. A. Cherry, and E. O. Frind, Migration of contaminants in groundwater at a landfill: A case study, 4, A natural-gradient dispersion test, *J. Hydrol.*, 63, 81-108, 1983.
- Winter, C. L., C. M. Newman, and S. P. Neumann, A perturbation expansion for diffusion in a random velocity field, *SIAM J. Appl. Math.*, 44(2), 411-424, 1984.
- E. A. Sudicky, Institute for Groundwater Research, Department of Earth Sciences, University of Waterloo, Waterloo, Ontario, Canada N2L 3G1.

(Received October 16, 1985;  
accepted September 9, 1986;  
revised September 15, 1986.)